ISBN: 978-3-95450-248-6 ISSN: 2673-5490 doi: 10.18429/JACoW-IPAC2025-WEPS022

PROGRESS ON EXPERIMENTAL EFFORTS TO INVESTIGATE CSR SHIELDING EFFECTS

G. Ha*, A. DeSimone, X. Lu[1], O. Ramachandran, B. N. Temizel Ozdemir
Northern Illinois University, DeKalb, USA
J. Power, Argonne National Laboratory, Lemont, USA
J. Qiang, Lawrence Berkeley National Laboratory
C. Huang, Los Alamos National Laboratory,
[1]also at Argonne National Laboratory, Lemont, USA

Abstract

A collaboration is underway to investigate the impact of Coherent Synchrotron Radiation (CSR) and shielding on beams of various shapes as they pass through a chicane. Experimental efforts have been made at the Argonne Wakefield Accelerator (AWA) facility. Currently, the facility is equipped with two identical doglegs with reversing quadrupoles that allow doglegs to function as a chicane, and manually adjustable shielding gaps. A 6.4-ps-long flattop laser pulse was generated using alpha-BBO crystals, and the linac phase was adjusted to either preserve the bunch length or slightly compress it through the chicane. While the expected beam behavior was observed during the initial experiment, the current chicane's exceptionally large R56 (=0.45 m) rendered it sensitive to modulations from the alpha-BBO configuration. We have confirmed a new beam-based tuning procedure for the BBO crystals and its effect on modulations. We present the summary of experimental efforts to date and outline future plans.

INTRODUCTION

Coherent Synchrotron Radiation (CSR) is a long-standing challenge in modern accelerator design. Various efforts have been made to understand CSR effects on the beam [1–3], to numerically estimate its impact [3–7], and to experimentally benchmark these predictions [8–10]. Among the remaining challenges, the shielding effect is particularly interesting as it directly modifies the radiation itself rather than focusing solely on its interaction with the beam. Experimental efforts in this direction include demonstrating the suppression of low-frequency components in the CSR spectra [11] and the reduction of CSR-induced energy spread from a single dipole magnet [12]. While these studies demonstrated the impact of shielding on the radiation or the beam under extremely small gaps, its impact on the beam in a compressor environment under nominal operating conditions remains unexplored.

We have modified the existing emittance exchange beamline at the Argonne Wakefield Accelerator (AWA) facility [13] to implement a chicane compressor with the dipole chambers equipped a pair of metallic plates whose gap size is tunable [14]. The AWA facility is among the most versatile platforms for generating on-demand beam conditions [15]. This environment makes it an ideal testbed for experimental investigations and benchmarking of CSR effects.

So far, we have designed and built the chicane compressor and conducted two initial experiments. These experiments revealed both challenges and promising results. In this paper, we describe the constructed beamline, provide example simulation results demonstrating the feasibility of CSR wake measurements, and discuss the encountered challenges, including sensitivity to initial laser modulation, along with the current status of the experiment.

CSR BENCHMARKING BEAMLINE AT ARGONNE WAKEFIELD ACCELERATOR

The AWA facility hosts an emittance exchange beamline consisting of two identical doglegs with a deflecting cavity in the middle. To minimize disruption to the existing facility layout, we added two quadrupole magnets between the doglegs to form a horizontal negative identity transport. This configuration enables flipping the beam instead of physically reconfiguring the beamline to realize a chicane. Except for the presence of strong horizontal focusing and vertical defocusing in the central region, the longitudinal dynamics of this reversed chicane are equivalent to those of a conventional C-type chicane. The beamline is also equipped with adjustable shielding gaps as shown in Fig. 1.

The overall layout of the CSR study beamline is shown in Fig. 2. The L-band injector can generate single bunch with charges ranging from 1 pC to 100 nC and bunch lengths corresponding to laser pulse durations from 0.3 to 6.4 ps (FWHM). This beam is accelerated to 44 MeV for CSR studies. The laser pulse length is typically adjusted using α-BBO crystals, but Gaussian pulse stacking with arbitrary spacing is also available.

Figure 1: Dipole chamber with adjustable shielding gap.

* gha@niu.edu

ISBN: 978-3-95450-248-6 ISSN: 2673-5490 doi: 10.18429/JACoW-IPAC2025-WEPS022

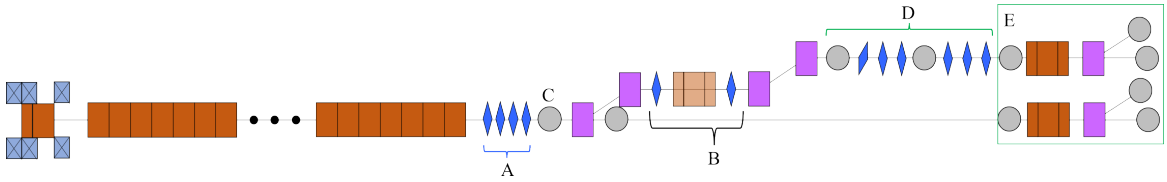

Figure 2: Experimental beamline layout. Brown boxes represent RF cavities; blue boxes indicate solenoids; blue diamonds are quadrupole magnets; purple boxes show rectangular dipole magnets; grey circles are diagnostic stations including slits or YAG screens.

The injector is followed by four quadrupole magnets in Region A, which control the entire transverse second moments (e.g., beam size and slope). The transversely controlled beam then enters the reversed chicane, which consists of two identical doglegs and the reversing quadrupole magnets in Region B. Region C, D, and E are diagnostic stations. Both C and D are equipped with vertical and horizontal slits mounted on motorized actuators. Thus, both slit-scan and quad-scan are available for measuring beam's transverse phase space. If one of the upstream quadrupoles is skewed, projection-based transverse phase space measurement can also be performed [16]. In addition, longitudinal phase space diagnostics are available both upstream and downstream of the chicane. This diagnostic section (Region E) consists of a deflecting cavity followed by a dipole magnet and screen. This configuration enables direct comparison of the initial and final transverse and longitudinal phase spaces to characterize the CSR impact.

Reversed Chicane and Reversing Quads

The principle of reversing quadrupole is analogous to that of a simple optical telescope: both reversing quads focus the beam in the horizontal plane, which flip the particles' horizontal position and momentum. However, due to the continuous horizontal focusing from reversing quads, the beam experiences strong vertical defocusing, which significantly tightens the vertical acceptance. In addition, any deviation from the nominal quadrupole settings can leave unwanted x-z coupling.

We simulated the impact of the incoming vertical slope and quadrupole strength errors. The results are shown in Fig. 3. To ensure proper beam transport, the incident vertical slope must remain within the range of 0 to 1 m^{-1}, and the quadrupole strengths must be controlled within $\pm 2\%$ of their design values. For this beamline, the nominal quadrupole gradient is 2.26 T/m, which requires strength control at the 0.04 T/m level. These requirements are within the achievable tuning capabilities of the AWA facility.

FEASIBILITY OF CSR WAKE MEASUREMENTS

It is well known that wakefields, which introduce time-dependent energy changes to the beam, can be reconstructed by comparing the longitudinal phase spaces with and without the wakefield [17, 18]. Similarly, we aim to experimentally

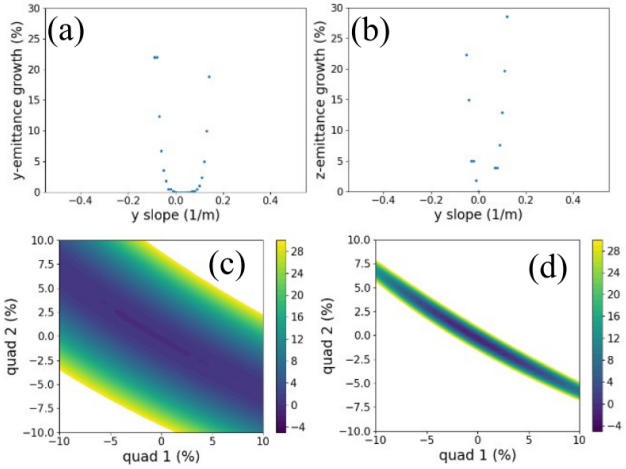

Figure 3: Vertical acceptance and quadrupole strength error tolerance of the reversed chicane.

retrieve the CSR wake by measuring the longitudinal phase space with and without the influence of CSR.

An example is shown in Fig. 4, which presents the longitudinal phase space distributions downstream of the chicane simulated using the General Particle Tracer (GPT) code. These are obtained via particle tracking with no CSR and with various shielding gap sizes. These simulations use a 10 nC bunch with near-zero longitudinal chirp at the entrance

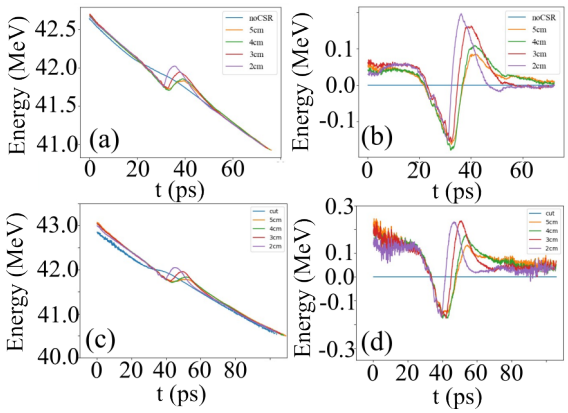

Figure 4: Simulated longitudinal phase space and the corresponding reconstructed CSR wakes for various shielding gap sizes. (a) and (b) show results with no-CSR for comparison, while (c) and (d) use the result from a slit with 2 mm opening.

ISBN: 978-3-95450-248-6 ISSN: 2673-5490 doi: 10.18429/JACoW-IPAC2025-WEPS022

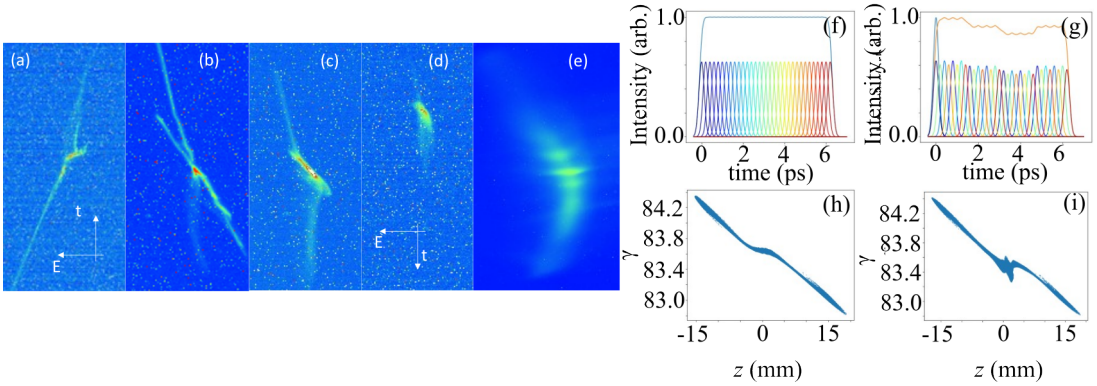

Figure 5: Effect of density modulation in the laser temporal profile on the downstream longitudinal phase space.

of the chicane. As in the standard wakefield reconstruction approach, subtracting the longitudinal correlations obtained at different gap sizes from the no-CSR case allows us to extract the CSR wake as shown in the panel (b).

A challenge in experimentally applying this method is the absence of a true "no-CSR" condition. To approximate this, we implemented a vertical slit with a 2-mm opening. As the beam passes through the slit, vertical clipping reduces the charge while largely preserving the horizontal and longitudinal distributions. Panels (c) and (d) show the results of this approach. The CSR wakefield corresponding to each gap size can still be reasonably reconstructed. It demonstrates the feasibility of this experimental approach.

EXPERIMENT #1 RESULTS AND ISSUES

In the first experiment, we observed longitudinal phase space patterns similar similar to those shown in Fig. 4; see panel (a) in Fig. 5. However, we also observed an unexpected X-shaped distribution shown in panel (b). Further analysis revealed that this structure originated from microbunching induced by density modulation in the laser's temporal profile.

The current chicane has an R_{56} of 0.45 m. Assuming sinusoidal modulations, a modulation amplitude greater than $1/kR_{56} \approx 1 \times 10^{-4}$ in δ-space is sufficient to induce critical or over-compression of the momentum modulation. We found that such modulation can readily arise from small angular errors in the alignment of the α-BBO crystals. Using simple ray optics, we estimated the changes in the laser's temporal profile caused by crystal angle errors, polarization-dependent mirror reflectivity, and the ordering of BBO crystals (e.g., thin-to-thick versus thick-to-thin). When all components are ideal, the laser profile forms a nearly perfect flattop (panel f), and the corresponding downstream longitudinal phase space exhibits a typical shape (panel h). However, when a 1° error is introduced in the thickest BBO crystal and mirror reflectivity shows a slight polarization dependence, the laser temporal profile changes significantly (panel g). It results longitudinal phase space develops strong microbunching (panel i).

This microbunching, when strongly compressed in the chicane, can combine with the main bunch envelope to form the X-like structure observed in panel (b). After identifying this cause, the angles of BBO crystals were further refined to reduce alignment errors. Improved longitudinal phase space images were obtained as shown in panel (c). However, residual microbunching remains and leads to localized saturation in the image. This microbunching was easily observable when the diagnostic slit was removed (panel e). Additionally, the phase space measured with the 2-mm slit exhibits a significantly shorter bunch length compared to the original. This issue has not yet been fully resolved.

EXPERIMENT #2 AND FUTURE PLAN

To work around the issues identified in Exp #1, we recently carried out Experiment #2, where we refined the BBO alignment procedure and introduced a laser splitter in the optical path. This setup allows the generation of two identical laser pulses—one containing the modulation and the other used to minimize it by introducing a temporal delay before recombination. This approach significantly improved the laser temporal profile and led to promising results shown in Fig. 6.

Unfortunately, due to an unexpected hardware issue, we were unable to complete the full data set acquisition including measurements at various shielding gaps. This measurement will be resumed in the near future.

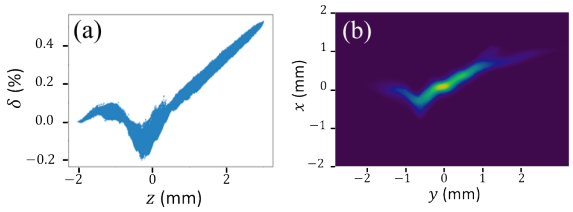

Figure 6: Simulated and measured longitudinal phase space from Experiment #2. Panel (b) shows raw screen image of the longitudinal phase space diagnostics. y and x correspond to z and δ, respectively.

ACKNOWLEDGMENTS

This work is supported by the U.S. Department of Energy, Office of Science, Office of High Energy Physics under Award DE-SC0024445 and the Contract No. DE-AC02-06CH11357.

ISBN: 978-3-95450-248-6 ISSN: 2673-5490 doi: 10.18429/JACoW-IPAC2025-WEPS022

REFERENCES

[1] Y. S. Derbenev, J. Rossbach, E. L. Saldin, and V. D. Shiltsev, "Microbunch radiative tail - head interaction", DESY, Hamburg, Germany, Tech. Rep. TESLA-FEL 1995-05, Sep. 1995. doi:10.3204/PUBDB-2018-04128

[2] P. Emma and G. V. Stupakov, "CSR wake for a short magnet in ultrarelativistic limit", in *Proc. EPAC'02*, Paris, France, pp. 1479–1481, 2007. https://jacow.org/e02/papers/WEPRI029.pdf

[3] Z. Huang and K.-J. Kim, "Formulas for coherent synchrotron radiation microbunching in a bunch compressor chicane", *Phys. Rev. ST Accel. Beams*, vol. 5, no. 7, p. 074 401, 2002. doi:10.1103/PhysRevSTAB.5.074401

[4] M. Dohlus and T. Limberg, "Emittance growth due to wake fields on curved bunch trajectories", *Nucl. Instrum. Methods Phys. Res., Sect. A*, vol. 393, no. 1, pp. 494–499, 1997. doi:10.1016/S0168-9002(97)00552-4

[5] M. Dohlus, A. Kabel, and T. Limberg, "Efficient field calculation of 3d bunches on general trajectories", *Nucl. Instrum. Methods Phys. Res., Sect. A*, vol. 445, no. 1, pp. 338–342, 2000. doi:10.1016/S0168-9002(00)00139-X

[6] M. Borland, "Simple method for particle tracking with coherent synchrotron radiation", *Phys. Rev. ST Accel. Beams*, vol. 4, no. 7, p. 070 701, 2001. doi:10.1103/PhysRevSTAB.4.070701

[7] I. V. Bazarov and T. Miyajima, "Calculation of coherent synchrotron radiation in General Particle Tracer", in *Proc. EPAC'08*, Genoa, Italy, pp. 118–120, 2008. https://jacow.org/e08/papers/MOPC024.pdf

[8] B. Beutner, W. Decking, M. Dohlus, T. Limberg, and M. Roehrs, "Beam Dynamics Experiments and Analysis on CSR Effects at FLASH", in *Proc. FEL'06*, Berlin, Germany, Aug.-Sep. 2006, pp. 56–58. https://jacow.org/f06/papers/MOPPH009.pdf

[9] S. Di Mitri, C. Venier, R. Vescovo, and L. Sturari, "Wakefield benchmarking at a single-pass high brightness electron linac", *Phys. Rev. Accel. Beams*, vol. 22, no. 1, p. 014 401, 2019. doi:10.1103/PhysRevAccelBeams.22.014401

[10] M. Shimada *et al.*, "Experimental exploration of compressed beam dynamics in an energy recovery linac with comparison to simulations", *Phys. Rev. Accel. Beams*, vol. 26, no. 3, p. 030 102, 2023. doi:10.1103/PhysRevAccelBeams.26.030102

[11] R. Kato *et al.*, "Suppression and enhancement of coherent synchrotron radiation in the presence of two parallel conducting plates", *Phys. Rev. E*, vol. 57, no. 3, pp. 3454–3460, 1998. doi:10.1103/PhysRevE.57.3454

[12] V. Yakimenko, M. Fedurin, V. Litvinenko, A. Fedotov, D. Kayran, and P. Muggli, "Experimental observation of suppression of coherent-synchrotron-radiation–induced beam-energy spread with shielding plates", *Phys. Rev. Lett.*, vol. 109, no. 16, p. 164 802, 2012. doi:10.1103/PhysRevLett.109.164802

[13] G. Ha *et al.*, "Precision control of the electron longitudinal bunch shape using an emittance-exchange beam line", *Phys. Rev. Lett.*, vol. 118, no. 10, p. 104 801, 2017. doi:10.1103/PhysRevLett.118.104801

[14] G. Ha, M. E. Conde, J. G. Power, and E. E. Wisniewski, "CSR shielding effect in dogleg and EEX beamlines", in *Proc. IPAC'18*, Vancouver, Canada, Apr.-May 2018, pp. 1498–1500. doi:10.18429/JACoW-IPAC2018-TUPMK005

[15] M. E. Conde *et al.*, "Research Program and Recent Results at the Argonne Wakefield Accelerator Facility (AWA)", in *Proc. IPAC'17*, Copenhagen, Denmark, May 2017, pp. 2885–2887. doi:10.18429/JACoW-IPAC2017-WEPAB132

[16] G. Ha, J. G. Power, E. E. Wisniewski, W. Liu, and M. Conde, "Single-shot measurement of transverse second moments using the projection method", *Phys. Rev. Accel. Beams*, vol. 24, no. 1, p. 012 802, 2021. doi:10.1103/PhysRevAccelBeams.24.012802

[17] Q. Gao *et al.*, "Single-shot wakefield measurement system", *Phys. Rev. Accel. Beams*, vol. 21, no. 6, p. 062 801, 2018. doi:10.1103/PhysRevAccelBeams.21.062801

[18] Q. Gao *et al.*, "Observation of high transformer ratio of shaped bunch generated by an emittance-exchange beam line", *Phys. Rev. Lett.*, vol. 120, no. 11, p. 114 801, 2018. doi:10.1103/PhysRevLett.120.114801